Chemical Geology 339 (2013) 43–51

Contents lists available at SciVerse ScienceDirect

Chemical Geology

journal homepage: www.elsevier.com/locate/chemgeo

Noble gas radionuclides in Yellowstone geothermal gas emissions: A reconnaissance

R. Yokochi [a,b,*], N.C. Sturchio [b], R. Purtschert [c], W. Jiang [d], Z.-T. Lu [d,e], P. Mueller [d], G.-M. Yang [d,f], B.M. Kennedy [g], Y. Kharaka [h]

[a] Department of Geophysical Sciences, The University of Chicago, Chicago, IL 60637, USA
[b] Department of Earth and Environmental Sciences, University of Illinois at Chicago, Chicago, IL 60607, USA
[c] Climate and Environmental Physics, Physics Institute, University of Bern, Sidlerstrasse 5, 3012 Bern, Switzerland
[d] Physics Division, Argonne National Laboratory, Argonne, IL 60439, USA
[e] Department of Physics and Enrico Fermi Institute, The University of Chicago, Chicago, IL 60637, USA
[f] Hefei National Laboratory for Physical Sciences at the Microscale, University of Science and Technology of China, Hefei, Anhui 230026, China
[g] Center for Isotope Geochemistry, Lawrence Berkeley National Laboratory, Berkeley, CA 94720, USA
[h] U.S. Geological Survey, Menlo Park, CA 94025, USA

ARTICLE INFO

Article history:
Accepted 23 September 2012
Available online 1 October 2012

Keywords:
Noble gas radionuclides
Yellostone National Park
Fluid Residence Time

ABSTRACT

A reconnaissance investigation of noble gas radionuclides (^{39}Ar, ^{81}Kr, and ^{85}Kr) in gas emissions from several geothermal features at Yellowstone National Park was performed to explore tracer applications of these nuclides in an active hydrothermal system. Prior studies of the Yellowstone system using stable noble gas isotopes show that the thermal fluids contain a mixture of atmospheric, mantle, and crustal components. Noble gas radionuclide measurements provide complementary chronometric information regarding subsurface residence times of thermal fluids, from decay of ^{81}Kr and ^{85}Kr as well as in situ production and release of nucleogenic ^{39}Ar and radiogenic ^{40}Ar* in the reservoir rock. Argon-39 isotopic abundances in air-corrected samples exceed those of atmospheric Ar by 705 to 1217%, indicating substantial Ar contribution to thermal fluids by fluid–rock interaction. Upper limits on deep thermal fluid mean residence times, estimated from ^{39}Ar/^{40}Ar* ratios, are about 100 kyr for features in the Gibbon and Norris Geyser Basin areas, and is about 30 kyr in Lower Geyser Basin, with the key assumption that the fluid acquires its crustal component of Ar in Quaternary volcanic rock of the Yellowstone caldera. Input of crustal Ar from older aquifer rocks would reduce these apparent mean residence times. ^{81}Kr isotopic abundances in the gas samples yield upper limits on residence time that are consistent with those obtained from ^{39}Ar/^{40}Ar* ratios.

1. Introduction

The classic study of Craig et al. (1956) showed that waters from the hot springs and geysers of Yellowstone are composed primarily of local meteoric water. Yet there is little quantitative data on the subsurface residence times of meteoric water discharged by Yellowstone thermal features (Pearson and Truesdell, 1978; Rye and Truesdell, 2007). This paper describes a new approach to examine fundamental questions pertaining to the residence time and geochemical evolution of Yellowstone hydrothermal fluids through the measurement of a set of noble gas radionuclides (Table 1); ^{39}Ar (half-life = 269 years), ^{81}Kr (half-life = 229,000 years), and ^{85}Kr (half-life = 10.8 years). The properties, measurement methods, and environmental tracer applications of the noble gas radionuclides were reviewed recently (Collon et al., 2004). The available data on stable noble gas isotopes in Yellowstone thermal waters and gases (Mazor and Wasserburg, 1965; Mazor and Fournier, 1973; Kennedy et al., 1985, 1987, 1988; Hearn et al., 1990) provide a good framework for understanding the systematics of the noble gas radionuclides in Yellowstone thermal fluids, within the context of the geological, geophysical, and geochemical setting of Yellowstone National Park and the surrounding region (Fournier, 1989; Christiansen, 2001).

Mixing and boiling are important processes in the evolution of Yellowstone thermal waters (Truesdell and Fournier, 1976; Truesdell et al., 1977). Kennedy et al. (1985) showed that noble gases in Yellowstone thermal waters and gases are mixtures of three components: those dissolved in air-saturated recharge water (ASW), crustal radiogenic noble gases (^{4}He-enriched, from crustal rock), and magmatic noble gases (^{3}He-enriched). Because of the low concentration of He in air-saturated water, the ^{3}He/^{4}He ratio is a good indication of the relative proportions of magmatic and radiogenic noble gases in Yellowstone thermal fluids. Also, as shown by Kennedy et al. (1987), the He isotope ratio reflects the relative timing of boiling and dilution in shallow thermal water reservoirs: deep dilution favors retention of the magmatic ^{3}He/^{4}He ratio and the conversion of magmatic CO_2 to bicarbonate, resulting in

* Corresponding author at: Department of Geophysical Sciences, The University of Chicago, Chicago IL, 60637 USA.
E-mail address: yokochi@uchicago.edu (R. Yokochi).

0009-2541/$ – see front matter © 2012 Elsevier B.V. All rights reserved.
http://dx.doi.org/10.1016/j.chemgeo.2012.09.037

Table 1
Noble gas isotopes used as tracers in this study. Isotopic abundances are those in the atmosphere (Collon et al., 2004). The asterisk in $^{40}Ar^*$ represents radiogenic component as opposed to atmospheric one.

Isotope	Primary source	Isotopic abundance	Half life (years)	Indicator of:
^{3}He	Mantle	1.4×10^{-6}		Magmatic contribution
^{4}He	Crust	~1		Input from the crust
^{39}Ar	Atmosphere and crust	8.1×10^{-16}	269	Rate of gas Ar release from the crust to the fluid
$^{40}Ar^*$	Mantle and crust	≡0		Input from the crust
^{81}Kr	Atmosphere	5×10^{-13}	229,000	Age of ancient atmospheric component
^{85}Kr	Atmosphere	$\sim10^{-11}$	10.8	Contribution of modern atmosphere

relatively high $^{3}He/^{4}He$ and HCO_3/Cl ratios in the thermal water, whereas deep boiling results in loss of magmatic He and CO_2 to steam, with the resulting low water-phase He concentration relatively susceptible to isotopic dilution by radiogenic He from the volcanic aquifer rock. Near-surface boiling and mixing of atmospheric and radiogenic noble gases during ascent of the fluid (Hearn et al., 1990; Gardner et al., 2011; Chiodini et al., 2012; Lowenstern et al., 2012) or from exchange between air and condensate pools and hot springs also may contribute substantially to the total noble gas isotopic composition of a given sample (Kennedy et al., 1988).

Measurements of the noble gas radionuclides in Yellowstone thermal fluids reveal additional dimensions of the noble gas mixing process. First, because all of the water is essentially meteoric to begin with, it is recharged as air-saturated water with its full complement of atmospheric Ar and Kr isotopes, including cosmogenic ^{39}Ar (isotopic abundance $=8.1\times10^{-16}$, Loosli (1983)) and ^{81}Kr (isotopic abundance $=5\times10^{-13}$, Collon et al. (1997)), and with recharge within the past ~50–60 years, fissiogenic ^{85}Kr from nuclear fuel reprocessing (isotopic abundance $\sim3\times10^{-11}$, Winger et al. (2005)). This water resides for a considerable length of time underground as it travels down to and within a thermal water reservoir before it ascends toward the surface, during which radioactive decay of the initial atmospheric abundances of the noble gas radionuclides provides three separate chronometers having time scales given by their decay constants. If water boils en route to the surface, without mixing, it may have lost much of its initial complement of noble gas radionuclides, but their isotopic abundances will reflect subsurface residence time. In addition, water–rock interactions release noble gas isotopes from the rocks encountered by circulating fluids along their flowpaths. These rocks may contain a primary inventory of noble gases (i.e., those incorporated from degassing magma), as well as a secondary inventory of radiogenic and nucleogenic noble gas isotopes produced in situ, including ^{4}He from the U- and Th-decay series, ^{40}Ar (from decay of ^{40}K), ^{39}Ar from neutron capture by ^{39}K (Lehmann and Purtschert, 1997), and ^{85}Kr from spontaneous fission of ^{238}U. Mixing of waters having different residence times may occur, as well as addition of stable, radiogenic, and radioactive noble gas isotopes from magmatic emanations as well as crystalline rocks of different compositions and ages. Thus a complex mixture of noble gases is possible, and interpretation of the noble gas isotopic abundances in gas emissions at the surface in accordingly complicated. Knowledge of the isotopic abundances of all noble gases in each of the mixing components is needed to be able to deconvolute the mixtures and to obtain chronometric information (see Table 1).

Different thermal areas in Yellowstone exhibit contrasting geochemical characteristics that reflect their fluid flow paths and boiling/mixing histories. For example, Mud Volcano and Crater Hills in the eastern portion of the Yellowstone Caldera, and Gibbon Springs along the northern rim of the caldera near Norris Geyser Basin, are located where fluids may rise from depth through relatively impermeable tuffs without losing their dissolved noble gases or mixing with shallower fluids (Fournier, 1989). In contrast, most other Yellowstone thermal areas, especially those within Upper and Lower Geyser Basins in the western portion of the Yellowstone caldera, are located among permeable rhyolite flow breccias and glacial sediments where mixing of deep and shallow fluids is taking place (Kennedy et al., 1987), and the noble gas radionuclides in these fluids could be dominated by mixing of younger, shallow fluids. For this reconnaissance study, we selected three locations where steam and gas emissions emerge from the Lava Creek Tuff (a fumarole adjacent to Beryl Spring in the Gibbon Springs group near the northern rim of the caldera; Frying Pan Spring near Norris Geyser Basin; and a frying-pan (sizzling H_2O-saturated ground) near Mud Volcano along the southwest margin of the Sour Creek Dome), and one where gas emissions emerge as bubbles through a hot spring pool in Lower Geyser Basin (Ojo Caliente Spring, Fig. 1).

2. Methods

2.1. Sampling

Large quantities of Kr (~10 μL STP) and Ar (~500 mL STP) are required for determining the isotopic abundances of noble gas radionuclides (STP = standard ambient temperature and pressure, 25 °C and 1 bar). The geothermal gases at YNP consist predominantly of H_2O and CO_2, and it was necessary to collect 5000–15,000 l STP of bulk gas in order to obtain sufficient quantities of Ar and Kr. Because it is not practical to transport such large quantities of gas, we removed H_2O and CO_2 in the field, via condensation and chemisorption by a pelletized $Ca(OH)_2$–NaOH mixture (Sodasorb®), respectively. The design of the field sampling system used in this study is shown schematically in Fig. 2. A large (~50-cm diameter) Teflon funnel was placed over the emission source and the rim of the funnel was sealed from atmosphere by submerging in water or saturated regolith. A Teflon tubing of 1/2 in. diameter was tightly connected to the funnel outlet with a hose clamp and carried the gas emission through a large (12-l volume) Pyrex condenser bulb submerged in a cold water bath to remove water from the gas by condensation. The cooled, partially dehydrated gas with a reduced amount of H_2O was then pumped by a vacuum compressor through a large U-shaped steel tube (6.5 cm diameter, 2 m total length) filled with pellets of Sodasorb® CO_2 absorbent (which also removes other trace acid gases), and the residual gas was stored in a gas cylinder for transport to the laboratory. The field sampling system was equipped with a vacuum pump and pressure gauges in order to facilitate leak checking, monitoring the progress of CO_2 absorption, and determination of the quantities of residual gas obtained.

2.2. Analyses

Bulk gas composition was analyzed using a SRS-200 quadrupole mass spectrometer in dynamic mode at University of Illinois at Chicago (UIC). Noble gas abundances and isotopic compositions of He and Ar were measured at Lawrence Berkeley National Laboratory. Krypton was extracted from the bulk gas at UIC by cryogenic distillation and gas chromatography (Yokochi et al., 2008), and the isotopic abundances of radiokrypton were determined by ATTA-3 at Laboratory for Radiokrypton Dating, Argonne National Laboratory (Jiang et al., 2012). ATTA-3 is an efficient and selective atom counter based on the Atom Trap Trace Analysis method (Chen et al., 1999). It is capable of measuring both $^{81}Kr/Kr$ and $^{85}Kr/Kr$ ratios of environmental samples in the range of 10^{-14} to 10^{-10}. For ^{81}Kr-dating in the age range of 150 kyr–1500 kyr, the required sample size is 5–10 μL STP of krypton gas, which can be extracted from approximately 1000–10,000 L STP of non-condensible geothermal gas with 1 % nitrogen content. For ^{85}Kr-analysis of geothermal gas enriched in young meteoric component, the required sample size is generally a factor of 10 less. At present, the Laboratory for Radiokrypton Dating at Argonne has one atom trap in operation and can analyze 120 samples per year. The same instrument has also been used to measure $^{39}Ar/Ar$ ratios of

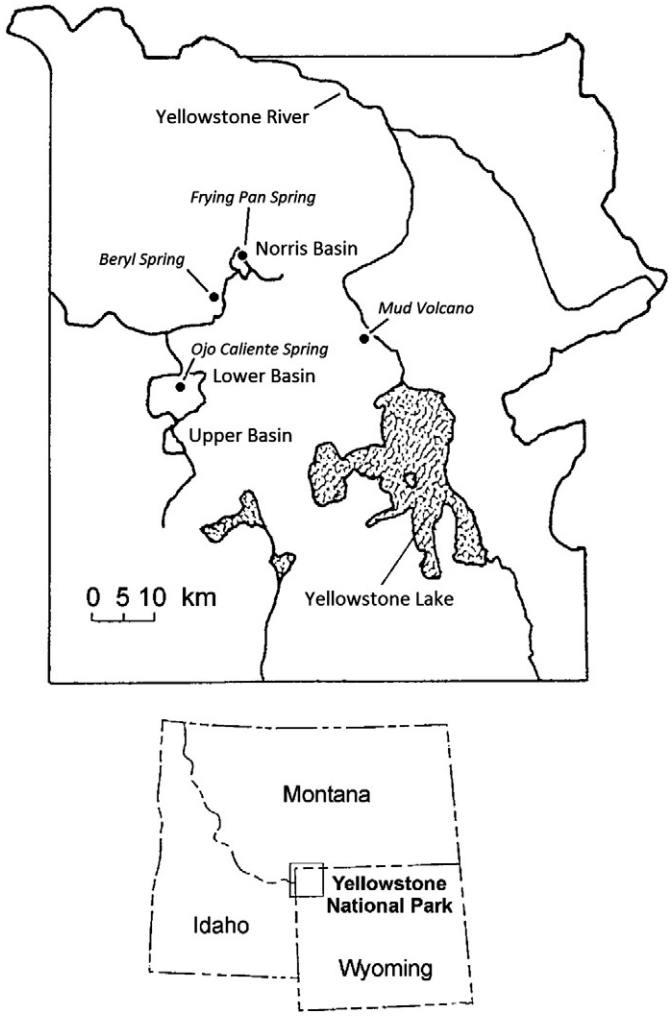

Fig. 1. Maps showing location of Yellowstone National Park in Wyoming–Montana–Idaho region (lower), and approximate locations of sampling sites in relation to major geographical features of Yellowstone National Park (upper).

environmental samples down to the 1×10^{-16} level (Jiang et al., 2011). However, the counting rate of ^{39}Ar needs to be improved by a factor of 10–100 before practical ^{39}Ar-dating can be realized using the ATTA method. The Kr-extraction residue was sent to the Physics Institute of the University of Bern, where Ar was purified and the ^{39}Ar abundance was determined by low-level anti-coincidence gas proportional counting (Loosli and Purtschert, 2005; Purtschert et al., 2012).

3. Results

Sampling sites, quantities of gas obtained, bulk gas chemical compositions, and noble gas isotopic compositions are listed in Table 2. Sample collection took place at four different locations: Beryl Spring, Mud Volcano, Frying Pan Spring and Ojo Caliente Spring. At the Frying Pan and Ojo Caliente springs, each gas sample was collected in a single gas cylinder. At the Beryl Spring, we obtained sample gas in two different cylinders, and the gases were combined for the analysis of noble gas radionuclides. At the fumarole near Mud Volcano, sample gas was also collected in two different cylinders, but because of valve corrosion during sampling, the gas in one of the cylinders was partially lost and contaminated with air during transport and storage. For the analysis of ^{39}Ar at Mud Volcano, the Ar in the two cylinders was combined in order to obtain a sufficient quantity of Ar for counting. For the analysis of radiokrypton, the gas in each of the two cylinders was purified and analyzed separately. The contribution of modern air due to valve leakage is corrected as described below.

Samples contained 6–14 % of O_2, which implies atmospheric contamination because geothermal gases at Yellowstone contain only trace amounts of oxygen according to previous studies (Bergfeld et al., 2011). It is likely that this atmospheric O_2 component was introduced during our large-volume gas sampling, either by entrainment of air (by the rapid flow of the gas near its vent) or by gas-stripping of air-saturated water due to the negative pressure gradient created by the vacuum compressor. The atmospheric contaminant most likely had modern noble gas radionuclide abundances. It is difficult to prevent such atmospheric contamination during sampling of large gas volumes, because of the irregular geometry of the natural vents and the unknown porosity, permeability, and saturation of the surrounding regolith. Nonetheless, we attempt to correct for the air contamination before discussing the history of the geothermal gas. For the purpose of correction, we assume that (i) the chemical compositions of gas samples reported in the literature for the same features that we sampled (Bergfeld et al., 2011) represent uncontaminated geothermal gas samples, and (ii) the atmospheric component can contaminate the sample either as unfractionated atmosphere (air) or as air-saturated water (ASW). Because the sample is deconvoluted into three end-members, three components (O_2, Ar and N_2) are sufficient to determine the mixing fraction of each end-member for these species.

In sample gases, the observed O_2/Ar ratios (subscripts "obs") resulting from mixtures of geothermal (subscripts "geo") and atmospheric (subscripts "atm", which is a mixture of air and ASW components with subscripts "air" and "ASW", respectively), can be expressed as:

$$\left[\frac{O_2}{Ar}\right]_{obs} = \frac{O_{2,atm}+O_{2,geo}}{Ar_{atm}+Ar_{geo}} = \frac{\left[\frac{O_2}{Ar}\right]_{atm} + \left[\frac{O_2}{Ar}\right]_{geo} \times \left[\frac{Ar_{geo}}{Ar_{atm}}\right]}{1+\left[\frac{Ar_{geo}}{Ar_{atm}}\right]} \quad (1)$$

Because Ar and O_2 have similar solubilities (S) in water, we first determined the proportion of atmospheric component (mixture of air and air-derived gas dissolved in water) relative to geothermal one for $S_{O_2}/S_{Ar} = 0.9 \pm 0.1$, covering the chemical compositions of the atmosphere and the range of solubilities at the local boiling point (93 °C) and salinities between 1000 and 1500 mg/l (Bergfeld et al., 2011). The chemical compositions of gas samples from (Bergfeld et al., 2011) were used as the geothermal end members, and are listed in Table 2. The atmospheric Ar component can be further deconvoluted into air and ASW components using contrasting solubilities of N_2 and Ar in water as:

$$\left[\frac{N_2}{Ar}\right]_{obs} = \frac{N_{2,atm}+N_{2,geo}}{Ar_{atm}+Ar_{geo}} = \frac{\left[\frac{N_2}{Ar}\right]_{atm} + \left[\frac{N_2}{Ar}\right]_{geo} \times \left[\frac{Ar_{geo}}{Ar_{atm}}\right]}{1+\left[\frac{Ar_{geo}}{Ar_{atm}}\right]} \quad (2)$$

$$\left[\frac{N_2}{Ar}\right]_{atm} = \frac{N_{2,air}+N_{2,ASW}}{Ar_{air}+Ar_{ASW}} = \frac{\left[\frac{N_2}{Ar}\right]_{air} + \left[\frac{N_2}{Ar}\right]_{ASW} \times \left[\frac{Ar_{ASW}}{Ar_{air}}\right]}{1+\left[\frac{Ar_{ASW}}{Ar_{air}}\right]} \quad (3)$$

The range of solubilities $S_{N_2}/S_{Ar} = 0.1 \pm 0.05$ was used for this calculation. This analysis showed that the contribution of ASW component is minor for all samples, thus the sample gas is considered as a mixture of atmosphere and a geothermal component as shown below.

The fraction of geothermal gas-derived Ar in our samples can be estimated as:

$$F_{Ar,geo} = \frac{\left[\frac{Ar_{geo}}{Ar_{air}}\right]}{1+\left[\frac{Ar_{geo}}{Ar_{air}}\right]} \quad (4)$$

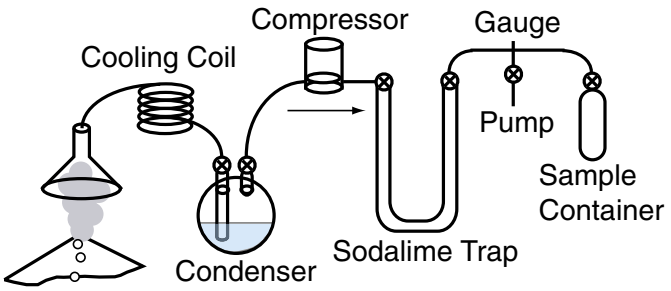

Fig. 2. Outline of on-site gas purification system utilized at Yellowstone National Park for sampling of CO_2-rich thermal gases. H_2O and CO_2 were removed in the field, via condensation and chemisorption by a pelletized $Ca(OH)_2$–NaOH mixture (Sodasorb®), respectively. The field sampling system was equipped with a vacuum pump and pressure gauges in order to facilitate leak checking, monitoring the progress of CO_2 absorption, and determination of the quantities of residual gas obtained (see Section 2.1 for detail).

Using the contributing fractions of air and geothermal Ar, it is possible to determine the Kr/Ar ratios of the geothermal gas components, as well as the fraction of the geothermal Kr.

$$\left[\frac{Kr}{Ar}\right]_{obs} = \frac{Kr_{air} + Kr_{geo}}{Ar_{air} + Ar_{geo}} = \frac{\left[\frac{Kr}{Ar}\right]_{air} + \left[\frac{Kr}{Ar}\right]_{geo} \times \left[\frac{Ar_{geo}}{Ar_{air}}\right]}{1 + \left[\frac{Ar_{geo}}{Ar_{air}}\right]} \quad (5)$$

$$F_{Kr,geo} = \frac{\left[\frac{Ar_{geo}}{Ar_{air}}\right] \times \left[\frac{Kr}{Ar}\right]_{geo}}{\left[\frac{Kr}{Ar}\right]_{Air} + \left[\frac{Ar_{geo}}{Ar_{air}}\right] \times \left[\frac{Kr}{Ar}\right]_{geo}} \quad (6)$$

Based on the estimated fractions of the atmospheric component, the modern air contribution was subtracted from the measured noble gas radionuclide abundances as:

$$\left[\frac{^{39}Ar}{\Sigma Ar}\right]_{geo} = \frac{\left[\frac{^{39}Ar}{\Sigma Ar}\right]_{obs} - F_{Ar,air} \times \left[\frac{^{39}Ar}{\Sigma Ar}\right]_{mod}}{F_{Ar,geo}} \quad (7)$$

$$\left[\frac{^{85}Kr}{\Sigma Kr}\right]_{geo} = \frac{\left[\frac{^{85}Kr}{\Sigma Kr}\right]_{obs} - F_{Kr,air} \times \left[\frac{^{85}Kr}{\Sigma Kr}\right]_{mod}}{F_{Kr,geo}} \quad (8)$$

The atmospheric component added by the valve leakage of the Mud Volcano sample is corrected in the same manner. The stable noble gas abundances and isotopic composition of the Mud Volcano sample could not be measured, unfortunately, due to accidental sample loss during processing in the mass spectrometry laboratory. The purified Kr sample from Beryl Spring was contaminated by atmosphere during storage in the laboratory. In this case, we could use the N_2/Kr ratio (~250) to determine the fraction of contaminating atmosphere assuming a unidirectional incorporation of ambient atmosphere due to the negative pressure gradient between the sample container and ambient atmosphere. Given the relatively low N_2/Kr ratio of the sample compared to the atmosphere ($\sim 7 \times 10^5$), more than 99.9% of measured Kr is from the sample gas. Thus measured isotopic abundance will be used for the discussion below.

The corrected results, including the mixing fractions of geothermal Ar and Kr, are shown in Table 3. In all samples, ^{85}Kr isotopic abundances were below atmospheric, whereas ^{81}Kr was atmospheric within 2σ uncertainty. The ^{39}Ar isotopic abundances were higher than atmospheric, indicating a significant subsurface contribution of ^{39}Ar (Purtschert et al., 2009).

Table 2
Chemical and isotopic compositions of gas samples from Yellowstone National Park. See Section 2.2 for the analytical methods. *F* values used for noble gases represent the ratio of those isotopes to ^{36}Ar normalized to that of the atmosphere. The chemical compositions of gas samples reported in the literature Bergfeld et al. (2011) taken from identical or nearby features without onsite purification were used for correcting the atmospheric contamination in our samples. The sample identifiers and compositions used for the correction are also shown at the bottom of this table as "Geothermal gas*".

Location	Beryl Spring		Mud Volcano		Frying Pan	Ojo Caliente	Air (frying pan)
Latitude	44°40′ 43.13″ N		44°37′ 23.60″ N		44°44′ 20.75″ N	44°33′ 46.60″ N	
Longitude	110°44′ 47.36″ W		110° 25′ 48.57″ W		110°42′ 02.84″ W	110°50′ 19.63″ W	
Sample Name	Beryl 2	Beryl 1	Mud Volcano 2	Mud Volcano 1	Frying Pan	Ojo Caliente	Air Frying Pan
Total gas (l STP)	15.0	16.9	11.9	36.7	28.3	71.5	86.2
Concentrations (%)							
CO_2	46(±2)	41(±2)	64(±3)	89(±4)	23(±1)		
N_2	46(±3)	51(±3)	29(±2)	9(±1)	63(±4)	81(±2)	79(±2)
Ar	0.85(±0.04)	0.94(±0.05)	0.41(±0.02)	0.12(±0.01)	0.83(±0.04)	1.12(±0.06)	0.96(±0.05)
O_2	5.85(±0.50)	5.25(±0.45)	6.04(±0.52)	0.49(±0.04)	11.85(±1.02)	13.93(±1.20)	20.13(±1.73)
CH_4	1.27(±0.07)	1.65(±0.09)	0.52(±0.03)	1.06(±0.06)	1.87(±0.10)	3.14(±0.17)	
Noble Gases							
F(^{4}He)		241.0 ± 13.7			84.8 ± 4.8	18.6 ± 1.1	
F(^{22}Ne)		0.77 ± 0.01			1.04 ± 0.01	0.98 ± 0.01	
F(^{84}Kr)		1.21 ± 0.02			0.98 ± 0.01	0.99 ± 0.01	
F(^{132}Xe)		1.52 ± 0.03			1.13 ± 0.03	1.10 ± 0.03	
^{3}He/^{4}He (R/Ra)		10.3 ± 0.2			4.4 ± 0.1	2.0 ± 0.0	
^{40}Ar/^{36}Ar		316.3 ± 1.5			300.0 ± 1.6		
^{39}Ar/Ar ($\times 10^{-15}$)		4.86 ± 0.486	3.00 ± 0.81		3.32 ± 0.486	4.86 ± 0.162	
% Modern		600 ± 60	370 ± 100		410 ± 60	600 ± 20	
^{81}Kr/Kr (Ra)		0.97 ± 0.09	0.93 ± 0.06		1.03 ± 0.07	1.06 ± 0.06	1.03 ± 0.06
^{85}Kr/Kr ($\times 10^{-11}$)		1.55 ± 0.094	1.78 ± 0.091		1.32 ± 0.067	1.12 ± 0.058	1.70 ± 0.079
^{85}Kr (dpm/cc)		51.1 ± 3.1	58.9 ± 3		43.6 ± 2.2	36.9 ± 1.9	56.2 ± 2.6
Geothermal gas*		**YL07-15**	**YL05-13**		**YL09-04**	**YL07-06**	
O_2/Ar		0.25 ± 0.13	0.08 ± 0.04		0.25 ± 013	0.18 ± 0.09	
N_2/Ar		44.4 ± 1.0	64.9 ± 1.5		39.8 ± 0.9	37.2 ± 0.8	

4. Discussion

4.1. Sources of noble gas radionuclides

Both ^{85}Kr and ^{39}Ar can have atmospheric and subsurface sources. We first constrain the origin of these radionuclides using the ^{85}Kr/^{39}Ar ratios. In the case of ^{39}Ar in our Yellowstone gas samples, the ^{39}Ar/Ar ratio is higher than that of modern atmosphere, thus it is evident that at least a fraction of ^{39}Ar was supplied to the fluid from rocks in the subsurface. The rocks that host the geothermal activity are relatively young (~640,000-yr Lava Creek Tuff and ~150,000-yr Central Plateau Member) rhyolites. Production rates of ^{85}Kr (^{85}P) and ^{39}Ar (^{39}P) were calculated based on a modified SLOWN code (Czubek, 1988, 1991), and the results are shown in Table 4. Based on these results, we obtain the ratio of production rates (^{85}P/^{39}P) of ~0.0018. If the system is closed for Ar and Kr, the concentrations (C) of these isotopes will reach production-decay equilibrium as:

$$\frac{dC}{dt} = P - \lambda \cdot C \tag{9}$$

Thus,

$$C(t) = \frac{P}{\lambda}\left(1 - e^{-\lambda t}\right) \tag{10}$$

where λ is the decay constant. This leads to an equilibrium ratio $C_{eq,^{85}Kr}/C_{eq,^{39}Ar} \sim 7 \times 10^{-5}$. In rocks losing Ar and Kr slowly at similar and constant rate with a rate constant $\alpha \ll 1$, the ^{85}Kr/^{39}Ar ratio is close to the equilibrium ratio, whereas it approaches the production ratio as the rate of loss increases (Fig. 3). If the transfer of these radionuclides from rock to fluid occurs, for example, due to the dissolution of minerals so that release is congruent, the ^{85}Kr/^{39}Ar ratio of the fluid inherits that of the rock for a fast and episodic transfer whereas this ratio will become lower for slow escape of noble gas radionuclides from rocks to the fluid phase (Yokochi et al., 2012). The ^{85}Kr/^{39}Ar ratios of sample gases prior to the atmospheric contamination during sampling can be calculated by:

$$\left[\frac{^{85}Kr}{^{39}Ar}\right]_{geo} = \left[\frac{^{84}Kr}{^{36}Ar}\right]_{obs} \times \frac{\left[\frac{^{84}Kr}{\Sigma Kr}\right]^{-1}}{\left[\frac{^{36}Ar}{\Sigma Ar}\right]^{-1}} \times \frac{F_{geo,Kr} \times \left[\frac{^{85}Kr}{\Sigma Kr}\right]_{geo}}{F_{geo,Ar} \times \left[\frac{^{39}Ar}{\Sigma Ar}\right]_{geo}} \tag{11}$$

The corrected ^{85}Kr/^{39}Ar ratios of our gas samples (Table 3) were significantly higher than those expected solely from subsurface production, suggesting a substantial contribution of modern atmosphere with ^{85}Kr/^{39}Ar ratio of 2.6 (at the time of the field sampling, Dubasov and Okunev (2010)). In other words, the subsurface nucleogenic ^{85}Kr signal is masked by that of modern atmosphere. We may therefore set a constraint on the possible contribution of young meteoric water (<60 yr) to the geothermal fluid using the measured ^{85}Kr isotopic abundance. Using this constraint, the abundance of the nucleogenic ^{39}Ar as well as the isotopic abundance of ^{81}Kr will be interpreted more rigorously.

4.2. Contribution of noble gases from young meteoric water to geothermal fluids

A study of tritium activities in Yellowstone thermal waters indicated that they consist of mixtures of about 10% relatively young water (<60 yr) with about 90% older water from a deep, well-mixed reservoir (>60 yr) (Pearson and Truesdell, 1978). Rye and Truesdell (2007) revisited this issue, and showed the feasibility of an age >10,000 yr for the older, deeper thermal water component, on the basis of an extensive set of stable isotope measurements of water from hot springs and rivers, along with chloride flux measurements and consideration of the likely volume of water contained within the deep reservoir of the Yellowstone caldera. A recent multitracer approach also demonstrated a mixing of CFCs- and tritium-bearing young water with old hydrothermal water (Gardner et al., 2011).

The lower-than-atmospheric isotopic abundance of ^{85}Kr in the Yellowstone gas samples can be interpreted as a result of (i) simple decay of ^{85}Kr in a purely young atmospheric component, or (ii) mixing of two components including a relatively young atmospheric component (up to modern) and an old component (^{85}Kr-dead), the proportions of which depend on the age of the younger component. The minimum fraction of the younger, atmospheric component (referred to as f_{mod}) as a function of its age is modeled and shown for each sample in Fig. 4 assuming that the older component contains no ^{85}Kr. The minimum fraction of modern component is calculated as:

$$f_{mod,Kr} = \left[\frac{^{85}Kr_{geo}}{\Sigma Kr}\right] / \left[\frac{^{85}Kr_{mod}}{\Sigma Kr}\right] \tag{12}$$

In the case of Beryl Spring, incorporation of this modern air component must have occurred quite recently, within only a few years of the sampling, presumably near surface. It dominates the Kr inventory ($f_{mod,Kr} > 0.8$). The contribution of such a modern atmospheric component appears minor at the Frying Pan and Ojo Caliente sites ($f_{mod,Kr} \sim 15\%$), whereas it could be larger if the age of the young component is a few tens of years (Fig. 4).

The difference in $f_{mod,Kr}$ values for the three samples may be related to the local surface topography of each site. Beryl Spring is situated at the base of a steep slope, and the sampled spring issues from acid-altered ground at the base of this slope. The slope above the spring is acid-altered up to a distance of about 20 m from the spring, and the ground is steaming which indicates diffuse emission of geothermal gas. The fumarole issues from regolith which is water-saturated, and the gas bubbles through water in a frying-pan type fumarole. It is likely that there is a substantial flux of water condensing from the geothermal steam on the hillside above the fumarole, from where it flows downhill toward Beryl Spring along with other cold water draining from higher

Table 3
Isotopic abundances of noble gas radionuclide after correcting the effect of atmospheric contamination presumably during sampling (the upper part of this table with subscript "geo", see Section 3). The middle section of this table shows maximum possible fractions of modern Ar and Kr ($f_{mod,Ar}$ and $f_{mod,Kr}$) in the geothermal gas (after corrected for the atmospheric contamination during sampling, see Section 4.1), as well as the fraction of radiogenic Ar derived from the crust as opposed to magma (Section 4.3.2). The chronological constraints based on noble gas radionuclides are shown at the bottom (Sections 4.3.1, 4.3.3 and 4.4). The equation used for calculating each parameter is also indicated.

Location	Beryl Spring	Mud Volcano	Frying Pan	Ojo Caliente	Method
^{40}Ar/^{36}Ar^{geo}	328 ± 5		308 ± 6	<298	
^{39}Ar/Ar$_{geo}$ (×10^{-15})	6.9 ± 0.95	5.7 ± 2.0	7.7 ± 1.9	9.9 ± 1.4	Eq. (7)
% Modern	846 (±117) %	705 (±248) %	947 (±228) %	1217 (±170) %	
^{85}Kr/Kr$_{geo}$ (×10^{-11})	1.49 ± 0.14		0.62 ± 0.32	0.39 ± 0.25	Eq. (8)
^{85}Kr dpm/cc	49.4 ± 4.5		20.5 ± 10.4	12.8 ± 8.3	
^{85}Kr/^{39}Ar$_{geo}$	0.350 ± 0.093		0.093 ± 0.058	0.047 ± 0.033	Eq. (11)
$F_{Ar,geo}$	0.67 ± 0.07	0.45 ± 0.08	0.37 ± 0.07	0.44 ± 0.07	Eq. (4)
$F_{Kr,geo}$	0.73 ± 0.11		0.35 ± 0.07	0.44 ± 0.06	Eq. (6)
$f_{mod,Ar}$	0.18 ± 0.02		0.19 ± 0.02	0.11 ± 0.01	Eq. (17)
$f_{mod,Kr}$	0.88 ± 0.09		0.37 ± 0.19	0.23 ± 0.15	Eq. (12)
$f_{^{40}Ar_c}$	0.22 ± 0.01		0.50 ± 0.01	0.71 ± 0.01	Eq. (20)
^{39}Ar/^{40}Ar$^{*}_{c}$ (Ra)	319 ± 40		443 ± 170	>1712	Eq. (22)
$t_{F,^{39}Ar}$(*kyr*)	157 ± 19.9		113 ± 43	<29	Eq. (16)
$t_{F,^{81}Kr}$(*kyr*)	<265		<83	<52	Eq. (26)

Table 4
Data for rock compositions near sample locations, and production of relevant noble gas isotopes. The chemical compositions of rocks are from Christiansen (2001).

Rocks	Lava Creek Tuff	Central Plateau Member
Relevant samples	Beryl Spring, Frying Pan, Mud Volcano	Ojo Caliente
Age years	640,000	160,000
K wt.%	4.3	4.3
Th ppmw	28.3	30
U ppmw	6.6	7.6
^{4}He atoms/g	2.76×10^{13}	3.04×10^{13}
^{40}Ar atoms/g	2.95×10^{12}	2.97×10^{12}
^{39}P atoms/g/yr	0.79	0.57
^{85}P atoms/g/yr	0.0011	0.0013
$C_{eq,^{39}Ar}$ atoms/g	308	222
$C_{eq,^{85}Kr}$ atoms/g	0.0170	0.0195
^{85}P/^{39}P	0.0014	0.0022
$C_{eq,^{85}Kr}/C_{eq,^{39}Ar}$	5.51×10^{-5}	8.80×10^{-5}
^{4}He/^{40}Ar*	9.4	10.2
$P_{^{39}Ar}/P_{^{40}Ar}$	2.12×10^{8}	3.81×10^{7}
^{39}Ar/^{40}Ar* (Ra)	1.3×10^{5}	9.2×10^{4}

on the slope. This cold water and condensate mixture may equilibrate with air and the high $f_{mod,Kr}$ value of the Kr in the gas sample from this site may result from gas-stripping of this mixture. The topography around Frying Pan and Ojo Caliente springs is more subdued and the shallow meteoric water that is encountered by the ascending gas may be older (thus having a lower ^{85}Kr/^{39}Ar ratio) or more slowly flowing (hence more thoroughly gas-stripped).

Krypton-85 is an excellent tracer for identifying the mixing of a young atmospheric component in geothermal gas. The fraction of noble gases contributed from young meteoric water apparently varies depending on the local topography and near-vent characteristics, and ^{85}Kr may enable quantification of this component. The fraction of young atmospheric component however depends on the age of this component, thus only lower limit can be set. It will be ideal to measure another tracer such as tritium in water vapor condensate in order to identify both the fraction and the age of the young atmospheric component.

4.3. Time scale of fluid residence time in the crust based on nucleogenic ^{39}Ar

4.3.1. Chronological method

A geochemical model for the evolution of nucleogenic ^{39}Ar and radiogenic ^{40}Ar* in coexisting rocks and fluids has been described recently (Yokochi et al., 2012). This model assumes that the abundance ratio of ^{39}Ar/^{40}Ar* in rocks and fluids is controlled by the Ar isotope production rates in the reservoir rock, the rock-to-fluid transfer of Ar isotopes, and decay of ^{39}Ar. Assuming a constant accumulation rate of ^{40}Ar* ($d^{40}Ar^*_F/dt \equiv a$. ^{40}Ar*$_F$, where subscript F represents fluid) with the reservoir rock ^{39}Ar/^{40}Ar* ratio of R_R, the concentration of ^{39}Ar in the fluid phase ($^{39}Ar_F$) varies as:

$$\frac{d^{39}Ar_F}{dt} = \Delta^{40}Ar^*_F \cdot R_R - \lambda_{39} \cdot {}^{39}Ar_F \tag{13}$$

After a time period, t_F, during which the fluid receives Ar from the rock, the amount of $^{40}Ar^*_F$ in the fluid is:

$${}^{40}Ar^*_F(t_F) = \Delta^{40}Ar^*_F \cdot t_F + {}^{40}Ar^*_F(0) \tag{14}$$

The ^{39}Ar and ^{40}Ar* ratio in the fluid (R_F) evolves as:

$$R_F(t_F) = \left[\frac{^{39}Ar}{^{40}Ar^*}\right]_F = \frac{\Delta^{40}Ar^*_F \cdot R_R \cdot \left(1-e^{-\lambda_{39}t_F}\right)/\lambda_{39} + {}^{39}Ar_F(0)\cdot e^{-\lambda_{39}t_F}}{\Delta^{40}Ar^*_F \cdot t_F + {}^{40}Ar^*_F(0)} \tag{15}$$

For a given R_R, a system that is more than ~1800 years since last contact with the atmosphere and has no significant ^{40}Ar* at the beginning (or can be corrected for magmatic ^{40}Ar* and atmospheric ^{39}Ar) provides the age as:

$$t_F = \frac{R_R}{R_F(t_F)\cdot\lambda_{39}} \tag{16}$$

Based on the chemical composition of the reservoir lithology and its age, the production rate of ^{39}Ar as well as the ^{39}Ar/^{40}Ar* ratio of the closed-system reservoir rock (R_R) can be estimated. The chemical compositions of the volcanic reservoir rocks from which the gas samples are emitted and the production rate of ^{39}Ar in these rocks are shown in Table 4. We estimate the closed system (^{39}Ar/^{40}Ar*) ratios of the reservoir rocks, Lava Creek Tuff and Central Plateau Member, of 1.3×10^5 and 9.2×10^4 Ra, respectively. In case Ar isotopes produced in older rocks beneath these reservoir rocks are incorporated into the fluid, these Ar source components also need to be considered. Other possible Ar sources include 2.1 Myr Huckleberry Ridge Tuff, as well as Wyoming Craton basement rocks ranging from 1.7 to 3.6 Gyr. Assuming the same chemical composition as Lava Creek Tuff for the Huckleberry Ridge Tuff, and assuming typical composition of continental crust for the Wyoming Craton rocks, we estimated the R_R ratios (Ra) to be 3.9×10^4, 142.1 and 35, respectively. Leeman et al. (1977) reported the occurrence of a Pb isotopic component derived from Mesozoic and Paleozoic sedimentary

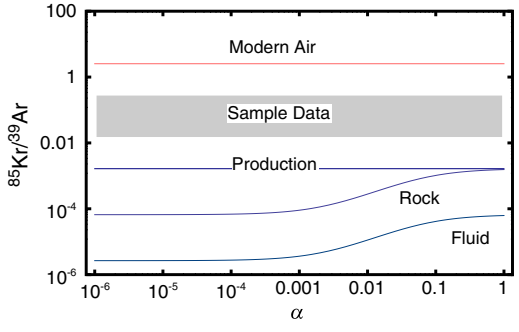

Fig. 3. The ^{85}Kr/^{39}Ar ratios of samples and possible end-members as a function of the release factor α (yr^{-1}) which is the fraction of noble gases lost from the mineral to the fluid phase. This ratio in rocks and minerals is close to that of production if the rate of Ar and Kr removal from the rock to the fluid phase is rapid (i.e. large α), and it decreases with α due to longer half life of ^{39}Ar. In the modern atmosphere, the ^{85}Kr/^{39}Ar ratio is much higher because of anthropogenic ^{85}Kr released during nuclear fuel reprocessing (see Section 4.1).

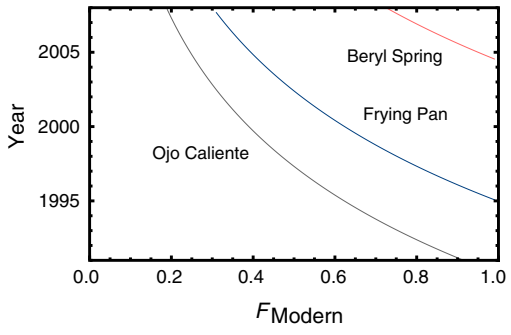

Fig. 4. The fraction of recent atmospheric component (*x*-axis) versus the time this component last equilibrated with the atmosphere (*y*-axis in year) based on the ^{85}Kr/Kr ratios (see Section 4.2).

rocks within Yellowstone hot-spring deposits, indicating long lateral travel paths from areas outside the Yellowstone caldera where sedimentary rocks outcrop at the surface, or the presence of these sedimentary rocks beneath the Yellowstone caldera. The R_R ratios of such component would be comparable to the Precambrian basement rocks. If there has been large partial Ar loss from the reservoir rock, these ratios would increase for each of the reservoirs, thus the age obtained by Eq. (16) using the closed system R_R value is a minimum estimate (see Yokochi et al. (2012) for detail).

4.3.2. Quantification of nucleogenic ^{39}Ar

The observed $^{39}Ar/\Sigma Ar$ ratio of the fluid needs to be corrected for the young atmospheric contribution of ^{39}Ar, as well as for magmatic $^{40}Ar^*$ in order to obtain the $R_F(t_F)$ value in the Eq. (16). The presence of ^{85}Kr in the Yellowstone gas samples implies that atmospheric ^{39}Ar also was incorporated into the thermal fluid with ^{85}Kr, and has not had enough time to decay. The contribution of minimum atmospheric ^{39}Ar can be constrained from the ^{85}Kr abundance, assuming modern atmospheric relative isotopic abundances for the contaminating atmospheric component as:

$$\left[\frac{^{85}Kr}{^{39}Ar}\right]_{obs} = \frac{^{85}Kr_{mod}}{^{39}Ar_{mod} + ^{39}Ar_{old}} = \frac{\left[^{85}Kr/^{39}Ar\right]_{mod}}{1 + \left[^{39}Ar_{old}/^{39}Ar_{mod}\right]} \quad (17)$$

Because of low ^{39}Ar isotopic abundance in the atmosphere, the fraction of modern air-derived ^{39}Ar constitutes only small fractions, between <1% and 11% (Table 3, $f_{mod,Ar}$).

The fluid gradually gains ^4He, ^{40}Ar and ^{39}Ar from the reservoir rocks during its residence in the crust. In order to obtain the crustal residence time of the fluid using the method described above, it is necessary to subtract the fraction of magmatic $^{40}Ar^*$ from the total $^{40}Ar^*$. Using the magmatic end-member composition of $^3He/^4He = 22$ R/Ra and $^4He/^{40}Ar^* \sim 1$ (Chiodini et al., 2012), and $^3He/^4He = 0.02$ R/Ra (Ballentine and Burnard, 2002) and $^4He/^{40}Ar^* \sim 4.08$ (Kennedy et al., 1987) for the crust, we determine the fraction of crustal $^{40}Ar^*$ relative to magmatic $^{40}Ar^*$ in each sample as:

$$\left[\frac{^3He}{^4He}\right]_{obs} = \frac{^3He_m + ^3He_c}{^4He_m + ^4He_c} = \frac{\left[\frac{^3He}{^4He}\right]_m + \left[\frac{^3He}{^4He}\right]_c \times \left[\frac{^4He_c}{^4He_m}\right]}{1 + \left[\frac{^4He_c}{^4He_m}\right]} \quad (18)$$

$$\left[\frac{^{40}Ar^*_c}{^{40}Ar^*_m}\right] = \left[\frac{^4He_c}{^4He_m}\right] \times \frac{\left[\frac{^4He}{^{40}Ar^*}\right]_c^{-1}}{\left[\frac{^4He}{^{40}Ar^*}\right]_m^{-1}} \quad (19)$$

$$f^{40}\mathbf{Ar}^*_\mathbf{c} = \frac{\left[\frac{^{40}Ar^*_c}{^{40}Ar^*_m}\right]}{1 + \left[\frac{^{40}Ar^*_c}{^{40}Ar^*_m}\right]} \quad (20)$$

The $^{39}Ar/^{40}Ar^*$ ratio of the sample is:

$$\left[\frac{^{39}Ar}{^{40}Ar^*}\right]_{obs} = \left[\frac{^{39}Ar}{\Sigma Ar}\right]_{obs} \times \left[\frac{^{40}Ar^*}{\Sigma Ar}\right]^{-1}_{obs} \quad (21)$$

The upper limit of this value prior to the fluid encounter with young meteoric water corrected for magmatic contribution is:

$$R_F = \left[\frac{^{39}Ar}{^{40}Ar*}\right]_{obs} \times \frac{1 - f^{39}Ar_{mod}}{f^{40}Ar*_c} \quad (22)$$

The fluids R_F values are 319 ± 40, 443 ± 170, and > 1712 times atmospheric value ($8.1 \times 10^{-16} \equiv$ Ra) for Beryl Spring, Frying Pan and Ojo Caliente, respectively. The Ojo Caliente sample did not show significant $^{40}Ar^*$, thus only the lower bound ratio using 3σ error limit was calculated.

4.3.3. Fluid residence time based on nucleogenic ^{39}Ar

The $[^{39}Ar/^{40}Ar^*]_F$ ratios calculated above translate to long estimated fluid residence times of 157 to 113 kyr for the gas samples from Beryl Spring and Frying Pan Spring, respectively (Eq. (16)), based on the closed-system evolution of $[^{39}Ar/^{40}Ar^*]_R$ ratios. A much younger upper limit of 29 kyr can be estimated for Ojo Caliente, as expected from the younger age of the reservoir rocks.

The estimated age would decrease significantly, for example for Beryl Spring, to 4.8×10^4, 170 and 42 years for the source rock ages of 2.1 Myr, 1.7 Gyr and 3.6 Gyr, respectively, if Ar is acquired from other source rocks (see Yokochi et al. (2012) for detail), and the multiple sources of Ar will lead to an intermediate age unless the relative contributions from each source can be resolved. This is an important uncertainty and additional constraints are needed to further refine these residence time estimates. Perhaps consideration of other solute isotopic ratios that are indicative of source rock contributions (e.g. Sr, Pb, Nd) could qualitatively constrain these inputs.

4.4. Implications of atmospheric ^{81}Kr abundance

Krypton-81 is produced only in the upper atmosphere by cosmic-ray interactions with atmospheric Kr, and its half-life is 229 kyr. While the near-atmospheric isotopic abundance of ^{81}Kr in our samples could simply indicate that the residence times of the geothermal fluids are less than about 20 kyr (5% 1σ uncertainty), the significant atmospheric contamination extends this age limit. The fraction of modern atmospheric contribution in our sample is given by:

$$\left[\frac{^{81}Kr_{old}}{^{81}Kr_{mod}}\right] = \frac{\left[\frac{^{81}Kr}{^{85}Kr}\right]_{obs} - \left[\frac{^{81}Kr}{^{85}Kr}\right]_{mod}}{\left[\frac{^{81}Kr}{^{85}Kr}\right]_{mod}} \quad (23)$$

$$F_{mod,^{81}Kr} = \frac{^{81}Kr_{mod} + ^{81}Kr_{old}}{^{85}Kr_{mod}} = \frac{\left[\frac{^{81}Kr}{^{85}Kr}\right]_{mod}}{\left[\frac{^{81}Kr}{^{85}Kr}\right]_{mod} + \left[\frac{^{81}Kr_{old}}{^{81}Kr_{mod}}\right] \times \left[\frac{^{81}Kr}{^{85}Kr}\right]_{mod}} \quad (24)$$

Using 5% uncertainty limit as:

$$\left[\frac{^{81}Kr}{\Sigma Kr}\right]_{obs} = F_{mod,^{81}Kr} \cdot \left[\frac{^{81}Kr}{\Sigma Kr}\right]_{mod} + \left(1 - F_{mod,^{81}Kr}\right) \cdot \left[\frac{^{81}Kr}{\Sigma Kr}\right]_{old} \quad (25)$$

For

$$\left[\frac{^{81}Kr}{\Sigma Kr}\right]_{obs} > 0.95 \cdot \left[\frac{^{81}Kr}{\Sigma Kr}\right]_{mod} \quad (26)$$

The upper limits of residence time are 265 kyr, 84 kyr and 52 kyr for Beryl Spring, Frying Pan and Ojo Caliente, respectively.

4.5. Summary and perspectives

Fig. 5 summarizes the age constraints from ^{81}Kr, ^{39}Ar and ^{85}Kr. The isotopic abundance of ^{81}Kr at Frying Pan indicates that the geothermal component is somewhat younger than the age estimates based on the closed system $^{39}Ar/^{40}Ar^*$ evolution of reservoir rock directly in contact with the fluids, which implies a contribution of subsurface-produced ^{39}Ar (and ^{85}Kr) from rocks beneath or surrounding the Lava Creek Tuff. The isotopic abundance of ^{85}Kr at Ojo Caliente suggests that the contribution of Ar isotopes from Precambrian basement rocks is minor. If the source of nucleogenic and radiogenic Ar isotopes is limited to the recent volcanic rocks associated with the magmatic activities within the caldera, the geothermal fluid has a long residence time in the

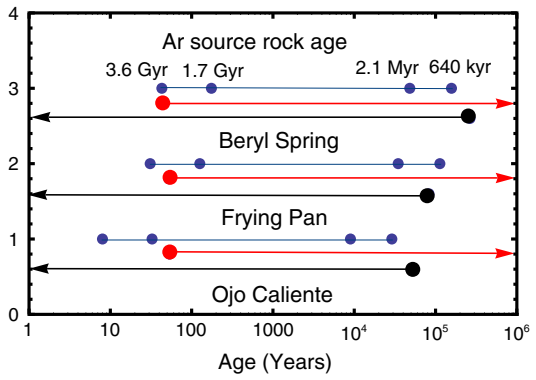

Fig. 5. Summary of the constraints on the fluid residence time based on ^{39}Ar (blue), ^{85}Kr (red) and ^{81}Kr (black). The numbers adjacent to the blue points represent the age of the source rock for ^{39}Ar assuming closed system ^{39}Ar/^{40}Ar* ratio.

crust, on the order of ~100 kyr for Beryl Spring and Frying Pan, and ~30 kyr for Ojo Caliente. The noble gas radionuclide chronometer will significantly improve by (i) decreasing the degree of atmospheric contamination during sampling, (ii) adding another constraint on the fraction and/or the age of the young meteoric component (e.g. tritium), and (iii) better knowledge on noble gas fluid–rock exchange.

5. Conclusion

Although difficult to sample and measure, the noble gas radionuclides provide a unique and valuable perspective on processes occurring in active hydrothermal systems. The short-lived isotope, ^{85}Kr (10.8 yr), is derived mostly from the atmosphere and is sensitive to near-surface mixing with young (<60 yr) groundwater or entrained air. The long-lived isotope, ^{81}Kr (229 kyr), is derived entirely from the atmosphere and gives an upper limit on the mean residence time of the thermal fluid. The intermediate-lived isotope, ^{39}Ar (269 yr), is derived both from the atmosphere and from nucleogenic production via ^{39}K(n, p)^{39}Ar reactions in reservoir rocks. There is a substantial excess of ^{39}Ar in the Yellowstone fluids indicating transfer of Ar isotopes from rocks to fluid in the subsurface. The ratio of ^{39}Ar/^{40}Ar* in thermal fluids can be related to the production rates of these isotopes in the rock and their transfer to the fluid, giving a quantitative estimate of the rock–fluid interaction time provided the age and composition of the rock are known and steady-state conditions are assumed (Yokochi et al., 2012). More complex models involving multiple reservoir rocks and/or episodic Ar release can be invoked but require additional constraints such as the isotopic compositions of other elements. Further investigation of noble gas radionuclides in Yellowstone, in conjunction with measurements of stable noble gas isotopes and other solutes, has the potential to reveal additional insights into the origin and evolution of thermal fluids as they pass through the entire hydrothermal cycle.

Acknowledgements

The U.S. National Science Foundation (EAR/PG-0838217, EAR/HS-0409756, and EAR/IF-0949404), the Donors of the American Chemical Society Petroleum Research Fund, the Postdoctoral Program in Environmental Chemistry of the Camille and Henry Dreyfus Foundation, and the U.S. Geological Survey are acknowledged for supporting this research. Analyses by Laboratory for Radiokrypton Dating at Argonne is supported by the Department of Energy, Office of Nuclear Physics, under contract DE-AC02-06CH11357. We are grateful to J. Lowenstern and T. Fischer for constructive comments, and to P. Gardner for his help during field sampling.

References

Ballentine, C.J., Burnard, P.G., 2002. Production, Release and Transport of Noble Gases in the Continental Crust. In: Porcelli, D., Ballentine, C.J., Wieler, R. (Eds.), 47. Noble gases in geochemistry and cosmochemistry. Rev. Mineral. Geochem., vol. 47. The Mineralogical Society Of America, Washington, pp. 481–538 (Jan., Ch. 12).
Bergfeld, D., Lowenstern, J., Hunt, A., Shanks III, W., Evans, W., 2011. Gas and Isotope Chemistry of Thermal Features in Yellowstone National Park, Wyoming. U.S. Geological Survey Scientific Investigations Report, 5012 (URL http://pubs.usgs.gov/sir/2011/5012/).
Chen, C.Y., Li, Y., Bailey, K., O'Connor, T., Young, L., Lu, Z.-T., 1999. Ultrasensitive isotope trace analyses with a magneto-optical trap. Science 286 (5442), 1139–1141.
Chiodini, G., Caliro, S., Lowenstern, J.B., Evans, W.C., Bergfeld, D., Tassi, F., Tedesco, D., 2012. Insights from fumarole gas geochemistry on the origin of hydrothermal fluids on the Yellowstone Plateau. Geochimica et Cosmochimica Acta 89, 265–278.
Christiansen, R., 2001. The Quaternary and Pliocene Yellowstone Plateau Volcanic Field of Wyoming, Idaho, and Montana. U.S. Geological Survey Professional Paper, 729–G (URL http://pubs.usgs.gov/pp/pp729g/).
Collon, P., Antaya, T., Davids, B., Fauerbach, M., Harkewicz, R., Hellstrom, M., Kutschera, W., Morrissey, D., Pardo, R., Paul, M., Sherrill, B., Steiner, M., 1997. Measurement of ^{81}Kr in the atmosphere. Nuclear Instruments and Methods in Physics Research B 123, 122–127.
Collon, P., Kutschera, W., Lu, Z.-T., 2004. Tracing noble gas radionuclides in the environment. Annual Review of Nuclear and Particle Science 54 (1), 39–67.
Craig, H., Boato, G., White, D., 1956. Isotopic geochemistry of thermal waters. Nuclear processes in Geologic Settings: National Research Council, Comm. Nuclear Sci., 19, pp. 29–38 (Ch. 5).
Czubek, J., 1988. SLOWN2.BAS Program for Calculation of the Rock Neutron Slowing Down Parameters. Tech. rep. Institute of Nuclear Physics, Krakow.
Czubek, J., 1991. Advances in absolute determination of the rock matrix absorption cross section for thermal neutrons. Nuclear Geophysics 5, 101–107.
Dubasov, Y.V., Okunev, N.S., 2010. Krypton and xenon radionuclides monitoring in the Northwest Region of Russia. Pure and Applied Geophysics 167 (4–5), 487–498.
Fournier, R., 1989. Geochemistry and dynamics of the Yellowstone National Park hydrothermal system. Annual Review of Earth and Planetary Sciences 17 (1), 13–53.
Gardner, W., Susong, D., Solomon, D., Heasler, H., Aug. 2011. A multitracer approach for characterizing interactions between shallow groundwater and the hydrothermal system in the Norris Geyser Basin area, Yellowstone National Park. Geochemistry, Geophysics, Geosystems 12 (8), 1–17.
Hearn, E., Kennedy, B., Truesdell, A., 1990. Coupled variations in helium isotopes and fluid chemistry: Shoshone Geyser Basin, Yellowstone National Park. Geochimica et Cosmochimica Acta 54 (11), 3103–3113.
Jiang, W., Williams, W., Bailey, K., Davis, A., Hu, S.-M., Lu, Z.-T., O'Connor, T., Purtschert, R., Sturchio, N., Sun, Y., Mueller, P., 2011. ^{39}Ar detection at the 10^{-16} isotopic abundance level with atom trap trace analysis. Physical Review Letters 106 (10), 1–4.
Jiang, W., Bailey, K., Lu, Z.-T., Mueller, P., O'Connor, T., Cheng, C.F., Hu, S.M., Purtschert, R., Sturchio, N., Sun, Y., Williams, W., Yang, G.-M., 2012. ATTA-3: an atom counter for measuring ^{81}Kr and ^{85}Kr in environmental samples. Geochimica et Cosmochimica Acta 91, 1–6.
Kennedy, B., Lynch, M., Reynolds, J., Smith, S., 1985. Intensive sampling of noble gases in fluids at Yellowstone: I. Early overview of the data; regional patterns. Geochimica et Cosmochimica Acta 49, 1251–1261.
Kennedy, B., Reynolds, J., Smith, S., Truesdell, A., 1987. Helium isotopes: lower geyser basin, Yellowstone National Park. Journal of Geophysical Research 92 (B12), 12477–12489.
Kennedy, B., Reynolds, J., Smith, S., 1988. Noble gas geochemistry in thermal springs. Geochimica et Cosmochimica Acta 52, 1919–1928.
Leeman, W., Doe, B., Whelan, J., 1977. Radiogenic and stable isotope studies of hot-spring deposits in Yellowstone National Park and their genetic implications. Geochemical Journal 11, 65–74.
Lehmann, B., Purtschert, R., 1997. Radioisotope dynamics — the origin and fate of nuclides in groundwater. Applied Geochemistry 12, 727–738.
Loosli, H., 1983. A dating method with ^{39}Ar. Earth and Planetary Science Letters 63, 51–62.
Loosli, H., Purtschert, R., 2005. Rare gases. In: Aggarwal, P., Gat, J., Froehlich, K. (Eds.), Isotopes in the Water Cycle: Past, Present and Future of a Developing Science. IAEA, Vienna, pp. 91–95.
Lowenstern, J.B., Bergfeld, D., Evans, W.C., Hurwitz, S., 2012. Generation and evolution of hydrothermal fluids at Yellowstone: insights from the Heart Lake Geyser Basin. Geochemistry, Geophysics, Geosystems 13 (1), 1–20.
Mazor, E., Fournier, R., 1973. More on noble gases in Yellowstone National Park hot waters. Geochimica et Cosmochimica Acta 37, 515–525.
Mazor, E., Wasserburg, G., 1965. Helium, neon, argon, krypton and xenon in gas emanations from Yellowstone and Lassen volcanic National Parks. Geochimica et Cosmochimica Acta 29, 443–454.
Pearson, F.J.J., Truesdell, A., 1978. Tritium in the waters of the Yellowstone National Park. U.S Geological Survey Open-File Report, pp. 327–329.
Purtschert, R., Yokochi, R., Sturchio, N., Kharaka, Y., Thordsen, J., 2009. Ar measurements on hydrothermal fluids from Yellowstone National Park. Geochimica et Cosmochimica Acta 73, A1060.
Purtschert, R., Yokochi, R., Sturchio, N., 2012. Kr-81 dating of old groundwater. In: Suckow, A. (Ed.), Dating Old Groundwater: A Guidebook. IAEA, Vienna, p. 400.
Rye, B.R.O., Truesdell, A.H., 2007. The Question of Recharge to the Deep Thermal Reservoir Underlying the Geysers and Hot Springs of Yellowstone National Park. In: Morgan, L. (Ed.), Integrated Geoscience Studies in the Greater Yellowstone Area - Volcanic, Tectonic, and Hydrothermal Processes in the Yellowstone Geoecosystem, profession Edition. U.S.Geological Survey, pp. 239–251.

Truesdell, A., Fournier, R., 1976. Conditions in the deeper parts of hot spring systems of Yellowstone National Park. U.S Geological Survey Open-File Report 76–428, pp. 1–22.
Truesdell, A.H., Nathenson, M., Rye, R.O., 1977. The effects of subsurface boiling and dilution on the isotopic compositions of Yellowstone Thermal Waters. Journal of Geophysical Research 82 (26), 3694–3704.
Winger, K., Feichter, J., Kalinowski, M.B., Sartorius, H., Schlosser, C., 2005. A new compilation of the atmospheric 85-Krypton inventories from 1945 to 2000 and its evaluation in a global transport model. Journal of Environmental Radioactivity 80 (2), 183–215.
Yokochi, R., Heraty, L.J., Sturchio, N.C., 2008. Method for purification of krypton from environmental samples for analysis of radiokrypton isotopes. Analytical Chemistry 80 (22), 8688–8693.
Yokochi, R., Sturchio, N., Purtschert, R., 2012. Determination of crustal fluid residence times using nucleogenic ^{39}Ar. Geochimica et Cosmochimica Acta 88, 19–26.